

## Mixing in Spacer-Filled Channels

C. Bayer<sup>1\*</sup>, H. Breisig<sup>2</sup>, M. Follmann<sup>3</sup>, C. Fritzmann<sup>4</sup> & T. Melin<sup>5</sup>

<sup>1-5</sup>AVT - Chemical Process Engineering, RWTH Aachen University, Germany

### ABSTRACT

Coated flat-sheet contacting devices are currently under development for a variety of membrane applications, e.g. in air conditioning [1], in the removal of CO<sub>2</sub> from fuel gases of biological origin [2] or in the elimination of trace organics from wastewater [3]. Generally, the relative take-up capacity of the stripping fluids is very large leading to low cross-flow velocities in the permeate channel. This undesirable consequence broadens the residence time distribution so that the stripping fluid is loaded unevenly. However, its effect can be reduced by enhancing lateral mixing. To quantify the mixing effects of spacers at different hydraulic conditions, this paper presents a suitable measurement method for lateral dispersion in spacer-filled channels. The measuring concept is based on mixing an acid and an alkaline stream, both marked with a pH indicator. The points in space where the pH indicator shifts its color are directly observed by photometric analysis. The resulting image is interpreted by transforming the axial space coordinate to a time coordinate, so that an analytical solution of Fick's Second Law can be fitted to the color-change front. The dispersion coefficient, which is a measure for lateral mixing in the spacer-filled channel, can be therewith obtained directly.

*Keywords:* Mixing, spacer, dispersion

### 1.0 INTRODUCTION

Flat-sheet contactor modules are currently under investigation in air conditioning [1] and in different extraction applications, such as fuel gas upgrading [2] and liquid/liquid extraction for wastewater treatment. In these cases, the solvents used have high take-up capacities, thus leading to low cross-flow velocities in the permeate. This broadens the residence time distribution leading to an uneven loading of the stripping fluids.

The impact of this may be reduced by turbulence-promoting devices such as spacers. These devices are net-type plastic fabrics with the main purpose of creating the gap between membranes for the fluid to flow through. Additionally, its interlaced structure enhances mixing. The better mixing created normal to the membrane has been widely documented and analyzed because it reduces

concentration polarization which limits many membrane applications.

Methods for quantifying the mixing behavior of spacers normal to the membrane surface are already in use, for instance the limiting current method [4]. In the design of the aforementioned modules, the quantification of the lateral mixing induced by spacers is also of significant interest. The limiting current method could be applied for this task, but it would mean designing a highly complex experiment. Instead, a very simple measurement principle is applied here. Mixing is marked by the color change of a pH-indicator induced by a neutralization reaction. This is done with the intention of determining approximate lateral dispersion coefficients and adequate conditions to run these measurements. Resulting dispersion coefficients and correlations can be subsequently used in CFD simulations in order to gain a better understanding of the behavior of flat-sheet contacting modules.

\* Corresponding to: C. Bayer (email: christoph.bayer@avt.rwth-aachen.de)

## 2.0 METHODS & MATERIALS

### 2.1 Theory

The measurement of the lateral dispersion coefficients is done by capturing photometrically the boundary between an acid and a basic solution flowing in parallel (both marked with a pH-indicator). The boundary, which represents the transition point of the indicator, is fitted to a solution of Fick's Second Law.

The theoretical description of the color-change boundary is based on Hartung [5]. He defined the normality ratio between the acid and the base as the ratio between the concentrations of the acid and the basic feed for univalent components:

$$X = \frac{n_A}{n_B} = \frac{c_{A0}}{c_{B0}} \quad (1)$$

The feed concentrations are defined as  $c_{A0}$  and  $c_{B0}$ , and a set of fictive concentrations (considering only diffusion without neutralization) as  $c_A$  and  $c_B$ . Furthermore, it is assumed that the diffusion coefficients of both species are identical, so that the relative concentrations sum up to one:

$$\frac{c_A}{c_{A0}} + \frac{c_B}{c_{B0}} = 1 \quad (2)$$

Considering that the condition for neutrality is  $c_A = c_B$ , equations (1) and (2) yield:

$$\frac{c_A}{c_{A0}} = \frac{X}{1 + X} \quad (3)$$

Equation 3 is then used as a constitutive equation in the solution of Fick's Second Law [6, page 63] as given in equation (4). Since this law described transient diffusion problems, an artificial time coordinate has to be defined. This is done by following a point along the iso-concentration curve described by the color-change boundary. Its velocity equals the constant flow velocity. The growing  $x$ -coordinate of this point divided by this velocity leads to the desired artificial time scale. This simplification is made assuming that the streamlines are not deflected on the length-scale of the test cell.

$$\frac{c(z, t)}{c_0} = \frac{z_0}{L} + \frac{2}{\pi} \sum_{n=1}^{\infty} \left( \frac{1}{n} \sin \left( \frac{n\pi z_0}{L} \right) \exp \left( \frac{-Dn^2\pi^2 t}{L^2} \right) \cos \left( \frac{n\pi z}{L} \right) \right) \quad (4)$$

$$\text{with and } t = \frac{x}{v} \text{ and } \frac{c(z, t)}{c_0} = \frac{X}{1 + X}$$

Finally, the infinite sum has to be approximated with a finite value in order to run a numerical calculation.  $L$  represents the width of the field in the test cell or the equivalent height of the 1D-diffusion cell.  $z_0$  is the center of the flow at  $x = 0$  or  $t = 0$ , which means that  $z_0/L$  equals 0.5. This yields the equation that is then fitted with MATLAB:

$$\frac{X}{1 + X} = 0.5 + \frac{2}{\pi} \sum_{n=1}^{\infty} \left( \frac{1}{n} \sin(0.5n\pi) \exp \left( \frac{-Dn^2\pi^2 x}{L^2 v} \right) \cos \left( \frac{n\pi z}{L} \right) \right) \quad (5)$$

### 3.0 EXPERIMENTAL SETUP

The first step in the design of the experiment was the construction of a test cell to obtain data (in this case as photographic images) without any disturbance in the flow field. On account of this, the test cell has to be manufactured in whole or in part with transparent materials in order to capture the color-change phenomenon taking place inside. The spacer to be tested here is a commercially available diamond-shaped spacer (Table 1).

**Table 1** Spacer dimensions

Spacer height $h_{SP}$	1 mm
Mesh size $L_M$	2 mm
Filament diameter $d_{FL}$	0.5 mm
Porosity $\epsilon$	0.8
Inner angle $\theta$	90°

The spacer is confined by two  $550 \times 200 \times 20$  mm plates that act as casing for the test cell. The upper plate is made of transparent acrylic glass and a white PTFE plate is used as bottom. This provides a good background for observing color changes in the flow field. Two threads are tapped on one side of the bottom plate to place the tube-fitting that will work as inlets (see Figure 1, left).

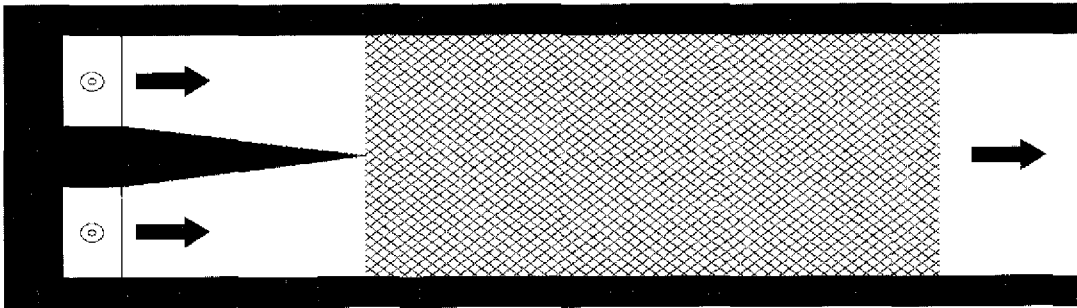


Figure 1 Schematic drawing of the test cell

A custom-cut silicone plate has the purpose of sealing the device on both long ends and at the inlets. The other end is left open as discharge. The triangular central stripe divides the two inlets and keeps both solutions apart until they reach the spacer-filled channel. Finally, the cell is assembled with screws in order to ensure sealing and keeping both plates pressed against the spacer.

The test cell is screened from surrounding light with a white blanket, so that any lighting changes in the environment do not affect the image capture. Approximately 30 cm above the test cell is a high resolution digital camera fixed to a support structure.

#### 4.0 EXPERIMENTAL PROCEDURE

The feed of the test cell consists of two inlet channels: one for an acid stream and the other for an alkaline stream. The solutions chosen for these experiments are hydrochloric acid HCl (aq) and caustic soda NaOH (aq), respectively. Both solutions were acquired from Merck in 1 mol/L concentration and diluted with deionized water to adjust the pH-value. To apply the previously mentioned model, a pH-indicator next to the neutrality point ( $\text{pH} = 7$ ) has to be used. Two common indicators meet this requirement: neutral red (red to yellow at  $\text{pH} 6.8 - 8$ ) and phenol red (yellow to red at  $\text{pH} 6.6 - 8$ ).

Both inlet channels are fed with the desired solutions set to a normality ratio of  $X = 3$ . Once the flow field has reached a steady state, a picture is taken and then processed with Photoshop and MATLAB. The first step enhances the contrast of the color-change boundary and creates a grayscale

image. MATLAB finds the boundary and fits its coordinates with equation (4), given the normality ratio and flow velocity. As a result, a dispersion coefficient is obtained.

## 5.0 RESULTS AND DISCUSSION

### 5.1 Indicator Performance

Selecting one of the two pH-indicators mentioned in the previous section was the first task at hand. A priori, two characteristics speak for the first indicator, neutral red. First, its theoretical transition pH-value is closer to the neutrality point, whereas phenol red has a slightly wider range. This is not nearly a sufficient criterion, since the pH changes abruptly around  $\text{pH} = 7$  and an exact transition cannot be seen. Thus, the assumption that the color-change front responds to the neutral point is applied here. The second and most important characteristic that points to neutral red, is its good solubility in water  $S_{NR} = 50 \text{ g/L} (@25^\circ\text{C})$ , compared to a very poor solubility of phenol red  $S_{PR} = 0.77 \text{ g/L} (@100^\circ\text{C})$ <sup>6</sup>.

At first glance, phenol red seems to have a better contrast in the test cell, but the processed images do not depict this fact (Figure 2). Phenol red presents more noise next to the boundary, which will ultimately lead to errors when fitting. This is because the MATLAB routine does not consider free black dots when searching for the boundary, but if the noise is next to it, it may yield a false position.

<sup>6</sup> Solubility values obtained from MERCK.

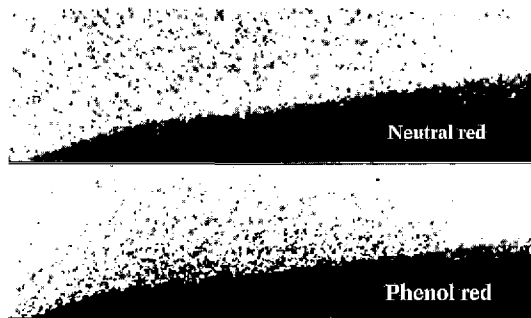


Figure 2 Processed images for both indicators

For the rest of the experiments to follow, the indicator neutral red is used, as it was proven more efficient.

## 6.0 INDICATOR CONCENTRATION

The indicator concentration should not affect the resulting curve at these low concentrations ( $c_{\text{ind}} \approx 10^{-4}$ – $10^{-5}$  mol/L). The fact that neutral red is a weak acid and that HCl and NaOH are given in concentrations of many orders of magnitude above  $c_{\text{ind}}$  dismisses any possible alteration of the desired pH.

Images are taken for four different indicator concentrations and compared in terms of the resulting mean dispersion coefficients  $D_M$  and the coefficient of variation between  $c_{v,D}$  for 10 samples (Table 3).

Table 3 Results for different indicator concentrations

	$c_{\text{ind}}$ [mol/L]	$D_M$ [cm <sup>2</sup> /s]	$c_{v,D}$ [-] <sup>a</sup>
1	$1.75 \cdot 10^{-5}$	0.138	0.0471
2	$3.5 \cdot 10^{-5}$	0.144	0.0383
3	$5.25 \cdot 10^{-5}$	0.137	0.0193
4	$7.0 \cdot 10^{-5}$	0.140	0.0186
		0.140	

<sup>a</sup> The coefficient of variation  $c_{v,D}$  equals the standard deviation  $\sigma_D$  divided by the mean value  $\bar{D}_M$

Results show that the coefficient of variation  $c_{v,D}$  of each experiment decreases along with an increasing indicator concentration. A higher  $c_{\text{ind}}$  yields a higher contrast, which reduces the undesired noise in the inactive (white) zone. These spots can distort the measured dispersion coefficient resulting in larger standard deviations and in larger coefficients of variation.

Additionally, the difference between the overall mean value and the mean values of each experiment is smaller than 3% and does not show any tendency with increasing  $c_{\text{ind}}$ . This means that the highest concentration has no significant influence on mixing, but it does improve the contrast and thus the image analysis. The highest concentration tested here may be then used without compromising the experiment. Beyond this point, higher concentrations are not taken into account.

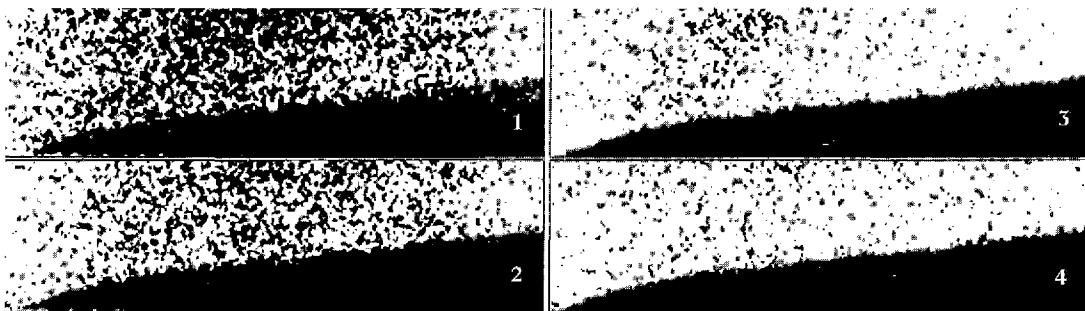


Figure 3 Processed images for different indicator concentrations

## 6.0 ACID/BASE STARTING CONCENTRATIONS

Keeping the normality ratio constant, the experiment is performed with different concentrations by changing the order of magnitude. If the starting concentrations of both acid and base are varied without modifying the normality ratio  $X$ , the resulting color-change boundary should not be affected.

Three different setups are considered here and also documented with 10 images. Results do not show any trend that may indicate a significant dependence of the dispersion coefficient on the concentration level of the solutions:

**Table 4** Results for different acid/base-concentrations

	$c_{A0}$ [mol/L]	$c_{B0}$ [mol/L]	$D_M$ [cm <sup>2</sup> /s]	$c_{v,D}$ [-]
1	0.003	0.001	0.123	0.1552
2	0.03	0.01	0.130	0.0491
3	0.3	0.1	0.129	0.0614

The mean dispersion coefficients present the same order of magnitude for all experiments run. These results are similar to those obtained when varying the indicator concentration, even taking into consideration that between series of experiments, the module was opened for cleaning and drying. The coefficient of variation in Experiment 1 is large compared to configurations 2 & 3. This dismisses lower concentrations. Higher concentrations do not seem to improve the quality of the images, so the second configuration (pH 1.5 vs. pH 12) is suitable for this application.

The application of Fick's Second Law approximates lateral mixing well, despite the inherent anisotropy of the spacer as seen in Figure 4.

## 7.0 CONCLUSIONS

A simple technique for quantifying lateral dispersion in a spacer-filled channel has been outlined in this paper. Further steps in the course of this study will aim at other experimental



**Figure 4** Processed image: Color-change boundary and fitted curve

parameters for defining trends and correlations for the lateral dispersion coefficient, which then can be used in CFD simulations.

#### ACKNOWLEDGEMENTS

This study is part of the EU Innowatech project (Contract No. 036882), which has been financially supported by the EU Commission within the thematic priority Global Change and Ecosystems of the Sixth Framework Program (FP6-2005-Global-SUSTDEV-2005-3.II.3.2).

#### REFERENCES

- [1] Usachov, V. V. *et al.* 2007. Membrane Contactor Air Conditioning System: Experience and Prospects. *Sep. Purif Technol.* 57: 502–506.
- [2] Gassanova, L. G., A. I. Netrusov, V. V. Teplyakov and M. Modigell. 2006 Fuel Gases from Organic Wastes using Membrane Bioreactors. *Desalination.* 198: 56–66.
- [3] INNOWATECH project website: <http://www.innowatech.org>
- [4] Li, F., W. Meindersma, A. B. de Haan, T. Reith. 2006. Experimental Validation of CFD Mass Transfer Simulations in Flat Sheet with Non-woven Net Spacers. *J. Membrane Sci.* 232: 19–30.
- [5] Hartung, Karl-Heinz. 1975. *Untersuchungen Technischer Mischvorgänge Mittels pH-Indikatoren.* Aachen: Mainz.
- [6] Crank, J. 1975. *The Mathematics of Diffusion.* 2nd ed. Oxford: Clarendon.